ORNL/TM-2013/398

COMPARISON OF FRICTIONAL HEATING MODELS

August 7, 2013

N. R. Davies* and P. J. Blau**

* **Department of Mechanical Engineering, University of Alabama – Tuscaloosa**

**** Materials Science and Technology Division, Oak Ridge National Laboratory**

ORNL/TM-2013/

Materials Science and Technology Division

COMPARISON OF FRICTIONAL HEATING MODELS

Nicholas R. Davies, Department Mechanical Engineering, University of Alabama - Tuscaloosa

Peter J. Blau, Materials Science and Technology Division, Oak Ridge National Laboratory

August 7, 2013

Prepared by
OAK RIDGE NATIONAL LABORATORY
Oak Ridge, Tennessee 37831-6283
managed by
UT-BATTELLE, LLC
for the
U.S. DEPARTMENT OF ENERGY
under contract DE-AC05-00OR22725

Contents

1.0 Abstract

The purpose of this work was to compare the predicted temperature rises using four well-known models for frictional heating under a few selected conditions in which similar variable inputs are provided to each model. Classic papers by Archard, Kuhlmann-Wilsdorf, Lim and Ashby, and Rabinowicz have been examined, and a spreadsheet (Excel™) was developed to facilitate the calculations. This report may be used in conjunction with that spreadsheet. It explains the background, assumptions, and rationale used for the calculations. Calculated flash temperatures for selected material combinations, under a range of applied loads and sliding speeds, are tabulated. The materials include AISI 52100 bearing steel, CDA 932 bronze, NBD 200 silicon nitride, Ti-6Al-4V alloy, and carbon-graphite material. Due to the assumptions made by the different models, and the direct way in which certain assumed quantities, like heat sink distances or asperity dimensions, enter into the calculations, frictional hearing results may differ significantly; however, they can be similar in certain cases in light of certain assumptions that are shared between the models.

2.0 Introduction

It has long been known that rubbing solid bodies together under a normal force can generate heat. In fact, that principle was used to start campfires for literally thousands of years. Despite this familiarity with frictional heating phenomena, there is lack of agreement among researchers on which properties to use, what assumptions to make, and how the input variables enter into the calculation. Two separate phenomena occur in the event of frictional heating, a rise in bulk temperature as well as a rise in flash temperature. The bulk temperature is considered to be the average temperature at the surface of a body, and its rise is attributed to the heat generated at the local contact points of friction diffusing into the near surface region. The flash temperature, on the other hand, is the temperature reached at the micro-scale points of contact, also called asperities, between the two bodies. In dry, non-lubricated frictional contact, the flash temperatures can be much higher than the bulk temperature. Flash temperatures can even approach the melting point of the materials under some conditions. By modeling the change in temperature experienced at asperities, predictions may be made about the wear, change in mechanical properties, or even indicate that melting occurs.

Historically, frictional heating models were developed based on assumptions about contact geometry, the partition of heat, and which material properties and geometric variables should be

included. Therefore, as the examples in this report show, there are non-trivial differences in the predicted temperatures from these models, despite similar material combinations, loads, and speeds of sliding.

3.0 Models Considered in this Study

Four frictional heating models were compared by incorporation into an Excel™ spreadsheet. The file-name for the work reproduced here is called "Friction Heating Calc_7Aug2013". The published references in which the models are described and the assumptions used in implementing them in the spreadsheet are listed below. Abbreviations in parentheses are used in the spreadsheet to identify each model.

3.1. Model 1: Archard Model (Arch)

3.1.1 *Reference*: Richard S. Cowan and Ward. O. Winer (1992) "Frictional Heating Calculations," in the ASM Handbook, Vol. 18, Friction, Lubrication, and Wear Technology, ASM International, Materials Park, OH, pp.39-43.

3.1.2 *Description of this Model*

The Archard model [1] is based on the seminal work of Blok [2] and Jaeger [3]. It is designed to determine the flash temperature developed through the friction of a self-mated combination of metals. The model seems to function fairly well under what might be considered non-severe sliding conditions, but appears rather unreliable for relatively high velocities and loads (i.e., normal forces). Four equations for determining the flash temperature are presented, one pair for the case where plastic deformation occurs, and the other pair is for elastic deformation. In each case, there is one equation modeling what Archard considered to be "low speed" friction. In that case, it is assumed that the heat flow is divided equally between the two surfaces. The second equation is for "high speed" friction, in which supposedly almost all of the heat flows into the counterface surface. In order to determine whether the friction is 'low' or 'high' speed, it is necessary to determine the Peclet number, a dimensionless quantity expressed as a function of velocity, contact geometry, and thermal diffusivity.

A problem arises from the discontinuous nature of the Archard model's equations. The equations for low speed friction are to be used when the Peclet number is less than 2, while the high speed equations are suited for a Peclet greater than 200. This leaves a gap where no clear relationship

exists. The approximation given by the model for conditions that fall into this gap is simply to average the results from the low and high speed equations. This causes what usually appears as a massive discontinuity on any graph used to represent results over a large range of sliding conditions. Examples of this jump in predicted temperature can easily be seen in the example tables provided: for example, in Table 5.1 in the "0.5 m/s Arch" column, where the predicted flash temperature ranges from 218 C to an absurd 11800 C as the Peclet number rises slightly above 2. The averaging approximation was used in that case. Based on the results reported in the example tables, it appears that any Peclet number between 2 and 200 produces an unreliable result. The user of the spreadsheet may wish to look at the 'Calculations' page, where the results for all three Peclet numbers are displayed, to determine which of them may present the most accurate result. Note that a Peclet number greater than 200 is rarely encountered in practice, and in all trial inputs, its use led to a temperature greater than the melting point of the material. Such results cast doubt on the viability of the equation for high speed sliding.

In contrast to the issues apparent with the higher Peclet numbers, the Archard model's results appear to be fairly reasonable for low speed friction. Another positive aspect of the model is its ability to determine flash temperature in circumstances of elastic deformation, where it requires the modulus of elasticity and Poisson's ratio in addition to the standard contact and material properties required by other models. A problem arises when attempting to model a dissimilar materials pair, however, because the model was designed for self-mated combinations having equal properties on each side of the sliding interface. In order to account for this missing functionality, the assumption has been made of using the properties of the counterface material for a number of variables, in the same manner as was done for the Kuhlmann-Wilsdorf model (described in Section 3.2), which shares many similarities with the Archard model and may have been inspired by it. While the assumptions made seem to be in agreement with the other models, the results of applying the Archard formulation are certainly not expected to be as accurate for dissimilar pairs.

3.1.3 *Major equations used in the calculation*.

Low speed plastic case $$\overline{T}_f = \mu \frac{\sqrt{\pi \cdot p_M}}{8k} W^{1/2} \cdot V_2 \quad (1)$$

High speed plastic case $$\overline{T}_f = 0.31 \mu \frac{(\pi \cdot p_M)^{3/4}}{(k \rho c)^{1/2}} W^{1/4} \cdot V_2^{1/2} \quad (2)$$

Low speed elastic case $$\overline{T}_f = 0.13\mu\left(\frac{1}{k}\right)\left(\frac{E_v}{R}\right)^{1/3} \cdot W^{2/3} \cdot V_2 \quad (3)$$

High speed elastic case $$\overline{T}_f = 0.36\mu\left(\frac{1}{\sqrt{k\rho c}}\right)\left(\frac{E_v}{R}\right)^{1/2} \cdot W^{1/2} \cdot V_2^{1/2} \quad (4)$$

Symbol definitions (units):

T_f = temperature increase due to flash heating (C)

V_2 = velocity (m/s)

W = normal force (N)

μ = coefficient of friction

p_M = hardness (Pa)

k = thermal conductivity (W/m*K)

E_v = (Elastic modulus [Pa]/(1- V_2^2)

ρ = density (kg/m^3)

R = undeformed radius of curvature of the slider (m)

C = specific heat (kJ/kg*K)

3.2. Model 2: Kuhlmann-Wilsdorf Model (Wil)

3.2.1 *Reference*: D. Kuhlmann-Wilsdorf (1985) "Flash Temperatures Due to Friction and Joule Heat at Asperity Contacts," *Wear*, **105**, pp. 187-198.

3.2.2 *Description of this Model*

Originally developed as part of a research project for the U.S. Navy on high current electrical contacts, the Kuhlmann-Wilsdorf model was designed to account for more sources of heat loss and gain than the Archard model, to which it is similar. An additional source of heat considered by this model, Joule heating from electric current passage, required many more inputs than those presented in equations 5 and 6, below, but that additional contribution has been omitted from the spreadsheet calculations in order to focus solely on the frictional heating contribution. The process for determining the real contact area of the asperities between the two rubbing substances is in fact identical to that of the Archard model, as both of them use the work of Blok and Jaeger for this calculation. Also similar is the Wilsdorf model's capability of calculating the frictional heating in cases of both plastic and elastic deformation.

Unlike the Archard model, however, the Wilsdorf model does allow for the calculation of the frictional heat between dissimilar materials. Additionally, the model not only allows for circular contact,

but also elliptical contact geometry. The Wilsdorf model also differs from other models in that it requires the Meyer hardness as opposed to the Brinell hardness, but due to the rarity of Meyer hardness data, the Brinell hardness number was used instead. Also of note is the use of kgf as opposed to Newtons in the original model. Due to the cancellation of the units, however, this distinction makes no difference in the end result.

3.2.3 *Major equations used in the calculation*.

Plastic case
$$ {}_{p}\Delta T_e = \frac{\pi f(Z,S)}{4\lambda_1}\left\{\mu v\left(\frac{PH_s}{N\pi}\right)^{1/2}\right\} \quad (5) $$

Elastic case
$$ {}_{E}\Delta T_e = \frac{\pi f(Z,S)}{4\lambda_1}\left\{0.29\mu v\left(\frac{P^2 E_{ave}}{r_2 N^2}\right)^{1/3}\right\} \quad (6) $$

Symbol definitions:

ΔT_e = temperature increase due to flash heating (C)

$_P$ = plastic deformation (subscript)

$_E$ = elastic deformation (subscript)

v = velocity (m/s)

P = normal force (N)

μ = coefficient of friction

H_s = hardness (Pa)

λ = thermal conductivity (W/m*K)

E_{ave} = average Young's Modulus (Pa)

N = number of contact spots

r_2 = undeformed radius of curvature (m)

$f(Z,S)$ = function describing the velocity and contact shape dependence of flash temperature

(Subscript 1 refers to counterface and subscript 2 refers to the asperity in this model.)

3.3. Model 3: Lim-Ashby Model (Ash)

3.3.1 *Reference*: S. C. Lim and M. F. Ashby (1987) "Overview No. 55: Wear-Mechanism Maps," Acta Metallurgica, Vol. 35, pp. 1-24.

3.3.2 *Description of this Model*

The Lim-Ashby model is similar in some respects to the Archard and Wilsdorf models, but has some key differences. While the previous two models take both contact and material properties into consideration, the Lim-Ashby model requires more feature size inputs, namely the linear thermal diffusion distance and the radius of a typical asperity, which both greatly affect this calculation. In Eqn. (8), the flash temperature is affected most significantly by the square root of the force multiplied by the velocity. This familiar piece of the equation (the friction force velocity product), however, is also multiplied by β, which is equal to the linear thermal diffusion distance divided by the radius of the sliding pin. The result of this is a relationship where the flash temperature is proportional to the value of β, giving immense importance to the geometric properties of the sliding body.

The Lim-Ashby model is the only model of the four with an ability to calculate both the bulk temperature (see Eqn.(7)) and the flash temperature (see Eqn. (8)). Note that the Ashby model expresses all temperatures in degrees Kelvin, whereas the other models use degrees Celsius. An additional capability of the Ashby model is the ability to find the flash and bulk temperatures when an oxide film is present; this functionality is reliant on the effective thermal conductivity, which will be that of the oxide film should one be present, or that of the counterface if no film is present. Like the Archard model, the Lim-Ashby model is intended for self-mated materials, but it takes an approach similar to the Archard model by using the values of the counterface's properties to present a better approximation for dissimilar material pairs. Essentially, this approximation treats the counterface as the original formula treats an oxide film.

3.2.3 *Major equations used in the calculation*.

Bulk temperature $$T_b = T_0 + \frac{\mu T^* \beta}{2 + \beta\left(\pi \bar{v}/8\right)^{1/2}} \bar{F}\bar{v} \tag{7}$$

Flash temperature $$T_f = T_b\left[1 - \left(\frac{\bar{F}}{N}\right)^{1/2}\right] + T_0\left(\frac{\bar{F}}{N}\right)^{1/2} + \frac{\mu T_c^* \beta}{2}\left(\frac{\bar{F}}{N}\right)^{1/2} \bar{v} \tag{8}$$

T_b = Bulk Temperature (°K)

T_f = Flash Temperature (°K)

T_0 = Initial (room) temperature (°K)

F = normalized force (N)

v = normalized velocity (m/s)

N = number of asperities

μ = coefficient of friction

*T** = equivalent temperature (°K)

β = linear thermal diffusion distance (m) / radius of pin (m)

3.4. Model 4: Rabinowicz Model (Rab)

3.4.1 *Reference*: Earnest Rabinowicz (1965) "Friction and Wear of Materials," John Wiley & Sons, New York, NY, pp. 87-93.

3.4.2 *Description of this Model*

The Rabinowicz 'model' was really intended to be a convenient, back-of-the-envelope approximation and not a rigorous treatment of the frictional heating problem. Still, it appears to provide reasonable estimates of temperature rise, albeit under limited circumstances. No effect of load or friction coefficient is incorporated in the model, and this significantly diminishes its usefulness. The reasoning behind neglecting load entirely in the calculation is actually supported to some extent by the other models, which are more drastically effected by a change in velocity than they are by a change in load. Despite this, the approximation presented by Rabinowicz is ineffective for extreme loads, as shown in the example calculations in Section 5.

3.4.3 *Major equations used in the calculation*.

$\Delta T = \frac{v}{2} \pm$ a factor of 3 (velocity in ft/min and temperature rise in °F) (9)

$\Delta T = 54.68v \pm$ a factor of 3 (velocity in m/s and temperature rise in °C) (10)

Symbol definitions:

$v =$ velocity (units of ft/min for Eqn. (9) and m/s for Eqn. (10))

$\Delta T =$ temperature rise due to flash heating (°F for Eqn. (9) and °C for Eqn. (10))

4.0 Computations and Organization of the Spreadsheet

The filename for the spreadsheet developed for use in this study is "Frictional Heating Calc_7 Aug 2013". It consists of five pages: "Inputs", "Results", "Calculations", "Utilities", and "Ex Tables". The input tables present all the raw variables used in the calculations in one place. The "Model Dependencies" chart to the right of the input table displays which models require which inputs. That allows the user to determine which models may or may not be used should the available input data be limited. The first input table is exclusively for material properties, with the asperity (slider) side listed as side 1 and the counterface listed as side 2. All inputs are displayed in SI units, except for the Brinell Hardness Number, which was left in terms of BHN (kgf/mm^2) due to its common use in the literature.

The second Inputs table is devoted to variables like load, speed, and contact geometry. Most of the required inputs are self-explanatory, but a few may require additional clarification. For example, the length and breadth of contact spots are used in the Wilsdorf model to allow for elliptical contact geometries. The number of apparent contact points (not asperities, but areas of nominal contact) is only

used in the Wilsdorf model. For the case of sliding pin-on-rotating disk friction configuration, that would be 1, while a four-pronged fork in place of the pin would be 4. The radius of an asperity, only used by the Lim-Ashby model, refers to the radius of the micro-scale points of contact between materials, which is dependent upon the material properties. In practice, the asperity radius is not accurately known. In these calculations, a value of 10^{-5}m (10 μm) was selected as a reasonable general estimate. The linear thermal diffusion distance, used by the Ashby model to represent the distance from the point of contact to the heat sink, has a direct scaling effect on the result and therefore should be selected carefully.

The 'Results' page layout was designed to enable convenient comparison of the inputs and results. If more detail is required, the 'Calculations' page provides as much clearly labeled relevant data as possible, so that the user may discern exactly where a value goes awry should the results appear unreasonable. It also permits one to view any results that were not presented based on default conditions (as for example with the Archard model). The 'Calculations' page also contains references to the cited source material, with all equations referenced by the same number they appear with in the source. It should also be noted that the models are color-coded to an extent across the 'Results', 'Calculations', and 'Ex Tables' pages to facilitate comparison.

The 'Utilities' page has been designed to provide the user with units conversions and a set of example material properties. The Unit Conversion Calculator allows for the conversion of U.S. customary units into their SI equivalents that are required as model inputs. The units to be converted should be placed in the left-hand orange box, but no user input should be entered in the results box because that would erase the embedded formulae. The Materials Properties Sheet contains all of the relevant material properties for the selected materials*. The melting point is provided due to the fact that if a material were to approach its melting point the frictional heating equations would be invalid.

Selected results for various material combinations, loads, and speeds are given in the 'Ex Tables' page (Example Tables) in the spreadsheet. The material combination is shown at the top left of the table, the velocity increases across columns, and the load increases down the rows. *All presented results are the rise in flash temperature in degrees Celsius for the described conditions*. Each column under velocity is divided into four color coded smaller columns, each corresponding to a different frictional heating model. Any cells that are presented as shaded with diagonal lines have results that exceeded the melting point of one of the two sliding partners, and of course that result is invalid. In addition to these tables, selected plots of various material combinations at a load of 10 N are given to enable a graphic comparison. All material properties used in example tables are taken from the 'Utilities' page, while all contact properties (other than Velocity and Load) are based on the data provided by Ashby and Wilsdorf, and are shown in the 'Inputs' page example that follows.

*Note: Provided properties data are 'handbook values' for illustrative purposes. The user should use thermo-physical and mechanical properties data for materials and contact geometries of current interest.

Table 1. "Inputs" page with example contact values

Input Tables				Model Dependencies:	Archard	Wilsdorf	Ashby	Rabino.
				Models with X require input for proper result.				
Material Properties	Symbol	Inputs	Units	Models with E only use input for Elastic Deformation				
Coefficient of Friction	μ	0.4	n/a		X	X	X	
Density - Side 1 (Slider)	ρ_1	4.43	x1000 kg/m^3 (g/cc)		X	X	X	
Density - Side 2 (Counterface)	ρ_2	7.81	x1000 kg/m^3 (g/cc)			X	X	
Thermal Conductivity - Side 1 (Slider)	k_1	6.7	W/m·°K		X	X	X	
Thermal Conductivity - Side 2 (Counterface)	k_2	42.7	W/m·°K			X	X	
Specific Heat - Side 1 (Slider)	c_1	0.526	kJ/kg ·°K		X	X	X	
Specific Heat - Side 2 (Counterface)	c_2	0.477	kJ/kg ·°K			X	X	
Modulus of Elasticity - Side 1 (Slider)	E_1	114	GPa		E	E		
Modulus of Elasticity - Side 2 (Counterface)	E_2	200	GPa		E	E		
Poisson Ratio	ν_p	0.3	n/a		E			
Effective Thermal Conductivity	k_c	42.7	W/m·°K				X	
Hardness, Brinell (softer side)	H	200	BHN (kgf/mm^2)		X	X	X	
					Archard	Wilsdorf	Ashby	Rabino.
Contact Properties	Symbol	Inputs	Units					
Normal Load	F	10	N		X	X	X	
Velocity	v	0.01	m/s		X	X	X	X
Radius of Curvature (Radius of Pin)	r	0.0015	m		E	E	X	
Length of Contact Spot	A	0.001	m			X		
Breadth of Contact Spot	B	0.001	m			X		
Number of Contact Spots	N	1	n/a			X		
Nominal Area of Contact	A_N	0.000007	m^2				X	
Radius of Asperity (typically 10^{-5})	r_a	0.00001	m				X	
Linear Diffusion Distance (Heatsink Distance)	l_b	0.008	m				X	
Heatsink Temperature (Room Temperature)	T	300	°K				X	
Deformation Type (Plastic or Elastic)	(P or E)	P	*Enter P or E*↵		X	X		

5.0 Sample Results and Comparisons

In these results, the material listed first is considered the slider and the material listed second is considered the counterface. All reported results are the Flash Temperature (Rise) (ΔT) in °C. Plots compare the models at different velocities under the same load. Results with temperatures above the melting point were omitted.

5.1 *Combination: AISI 52100 steel self-mated*.

Table 2. Comparison of Friction-Induced Temperature Rise for Self-Mated AISI 52100 Steel

Self-mated	0.01 m/s				0.05 m/s				0.1 m/s				0.5 m/s				1.0 m/s			
AISI 52100 Steel	Arch	Wil	Ash	Rab	Arch	Wil	Ash	Rab	Arch	Wil	Ash	Rab	Arch	Wil	Ash	Rab	Arch	Wil	Ash	Rab
1 N	1.38	1.38	5.82	0.55	6.89	6.83	29	2.73	13.8	13.5	58	5.47	68.9	63.1	290	27.3	138	116	580	54.7
10 N	4.36	4.33	7.41	0.55	21.8	21.1	36.4	2.73	43.6	41.2	72.5	5.47	218	169	360	27.3	5340	293	718	54.7
100 N	13.8	13.5	10.1	0.55	68.9	63.1	44.3	2.73	138	116	84.9	5.47	1.E+06	404	395	27.3	16000	645	775	54.7

5.2 *Combination: AISI 52100 Steel on Silicon Nitride Ceramic*

Table 3. Comparison of Friction-Induced Temperature Rise for AISI 52100 Steel on Silicon Nitride

AISI 52100 Steel on	0.01 m/s				0.05 m/s				0.1 m/s				0.5 m/s				1.0 m/s			
Silicon Nitride	Arch	Wil	Ash	Rab	Arch	Wil	Ash	Rab	Arch	Wil	Ash	Rab	Arch	Wil	Ash	Rab	Arch	Wil	Ash	Rab
1 N	2.51	2.04	10.6	0.55	12.6	10.2	52.9	2.73	25.1	20.2	106	5.47	126	95.9	528	27.3	251	181	1060	54.7
10 N	7.94	6.44	13.5	0.55	39.7	31.7	66.5	2.73	79.4	62	132	5.47	397	267	655	27.3	1180	476	1310	54.7
100 N	25.1	20.2	18.6	0.55	126	95.9	81.5	2.73	251	181	156	5.47	2900	672	723	27.3	2800	1100	1420	54.7

5.3 *Combination: AISI 52100 Steel on CDA 932 Bronze*

Table 4. Comparison of Friction-Induced Temperature Rise for AISI 52100 Steel on CDA 932 Bronze

AISI 52100 Steel on	0.01 m/s				0.05 m/s				0.1 m/s				0.5 m/s				1.0 m/s			
CDA 932 Bronze	Arch	Wil	Ash	Rab	Arch	Wil	Ash	Rab	Arch	Wil	Ash	Rab	Arch	Wil	Ash	Rab	Arch	Wil	Ash	Rab
1 N	0.72	0.83	2.03	0.55	3.6	4.11	10.1	2.73	7.21	8.11	20.1	5.47	36	37	100	27.3	72.1	66.6	201	54.7
10 N	2.28	2.61	2.46	0.55	11.4	12.7	11.7	2.73	22.8	24.4	23	5.47	1190	98.4	112	27.3	4540	160	222	54.7
100 N	7.21	8.11	5.08	0.55	36	37	19.2	2.73	72.1	66.6	34.5	5.47	5750	218	141	27.3	8230	340	266	54.7

5.4 *Combination: CDA 932 Bronze on AISI 52100 Steel*

Table 5. Comparison of Friction-Induced Temperature Rise for CDA 932 Bronze on AISI 52100 Steel

CDA 932 Bronze on	0.01 m/s				0.05 m/s				0.1 m/s				0.5 m/s				1.0 m/s			
AISI 52100 Steel	Arch	Wil	Ash	Rab	Arch	Wil	Ash	Rab	Arch	Wil	Ash	Rab	Arch	Wil	Ash	Rab	Arch	Wil	Ash	Rab
1 N	0.98	0.83	2.76	0.55	4.91	4.1	13.7	2.73	9.83	8.09	27.4	5.47	49.1	36.6	137	27.3	98.3	65.2	273	54.7
10 N	3.11	2.61	3.3	0.55	15.5	12.6	15.7	2.73	31.1	24.2	31	5.47	1550	96	151	27.3	5060	160	301	54.7
100 N	9.83	8.09	6.44	0.55	49.1	36.6	24.5	2.73	98.3	65.22	44.3	5.47	6410	221	185	27.3	9220	351	351	54.7

5.5 *Combination: AISI 52100 Steel on Titanium Alloy Ti-6Al-4V*

Table 6. Comparison of Friction-Induced Temperature Rise for AISI 52100 Steel on Titanium Alloy

AISI 52100 Steel on	0.01 m/s				0.05 m/s				0.1 m/s				0.5 m/s				1.0 m/s			
Titanium Alloy	Arch	Wil	Ash	Rab	Arch	Wil	Ash	Rab	Arch	Wil	Ash	Rab	Arch	Wil	Ash	Rab	Arch	Wil	Ash	Rab
1 N	5.86	1.59	24.7	0.55	29.3	7.87	123	2.73	58.6	15.6	246	5.47	7860	73.1	1230	27.3	11200	137	2462	54.7
10 N	18.5	4.99	31	0.55	92.6	24.4	153	2.73	185	47.3	306	5.47	14200	205	1520	27.3	20300	370	3046	54.7
100 N	58.6	15.6	38.3	0.55	7860	73.1	174	2.73	11200	137	338	5.47	25900	539	1620	27.3	37400	930	3210	54.7

5.6 *Combination: Titanium Alloy Ti-6Al-4V on AISI 52100 Steel*

Table 7. Comparison of Friction-Induced Temperature Rise for Titanium Alloy on AISI 52100 Steel

Titanium Alloy on	0.01 m/s				0.05 m/s				0.1 m/s				0.5 m/s				1.0 m/s			
AISI 52100 Steel	Arch	Wil	Ash	Rab	Arch	Wil	Ash	Rab	Arch	Wil	Ash	Rab	Arch	Wil	Ash	Rab	Arch	Wil	Ash	Rab
1 N	0.92	1.58	3.88	0.55	4.6	7.82	19.4	2.73	9.19	15.4	38.7	5.47	46	68.5	193	27.3	91.9	120	386	54.7
10 N	2.91	4.97	4.94	0.55	14.5	23.9	24.3	2.73	29.1	45.6	48.3	5.47	145	167	240	27.3	6220	272	478	54.7
100 N	9.19	15.4	6.73	0.55	46	68.5	29.6	2.73	91.9	120	56.6	5.47	7670	358	263	27.3	11300	535	517	54.7

5.7 *Combination: Self-Mated Carbon-Graphite*

Table 8. Comparison of Friction-Induced Temperature Rise for Self-Mated Carbon-Graphite

Self-mated	0.01 m/s				0.05 m/s				0.1 m/s				0.5 m/s				1.0 m/s			
carbon(70%)/graphite	Arch	Wil	Ash	Rab	Arch	Wil	Ash	Rab	Arch	Wil	Ash	Rab	Arch	Wil	Ash	Rab	Arch	Wil	Ash	Rab
1 N	1.07	1.06	3.33	0.55	5.33	5.22	16.6	2.73	10.7	10.2	33.1	5.47	53.3	43.7	165	27.3	2620	77.2	331	54.7
10 N	3.37	3.32	3.94	0.55	16.9	15.8	19.1	2.73	33.7	29.6	37.7	5.47	3310	108	186	27.3	4730	173	370	54.7
100 N	10.7	10.21	6.53	0.55	53.3	43.7	26.1	2.73	2620	77.2	48.4	5.47	6010	234	213	27.3	2650	362	411	54.7

NOTE: Upon inspection of the data in Tables 4 and 5, as well as 6 and 7, it is notable that the results differ in each pairing despite the fact that the same set of materials being tested. This may be attributed to the models distinguishing between the pin and counterface in the calculations. Thus, these results suggest that in pin-on-disk contact, frictional heating is not only dependent upon the materials used, but also upon which material is in a state of constant contact, and which is not.

5.8 *Graphical comparison of models for Self-Mated AISI 52100 Steel*

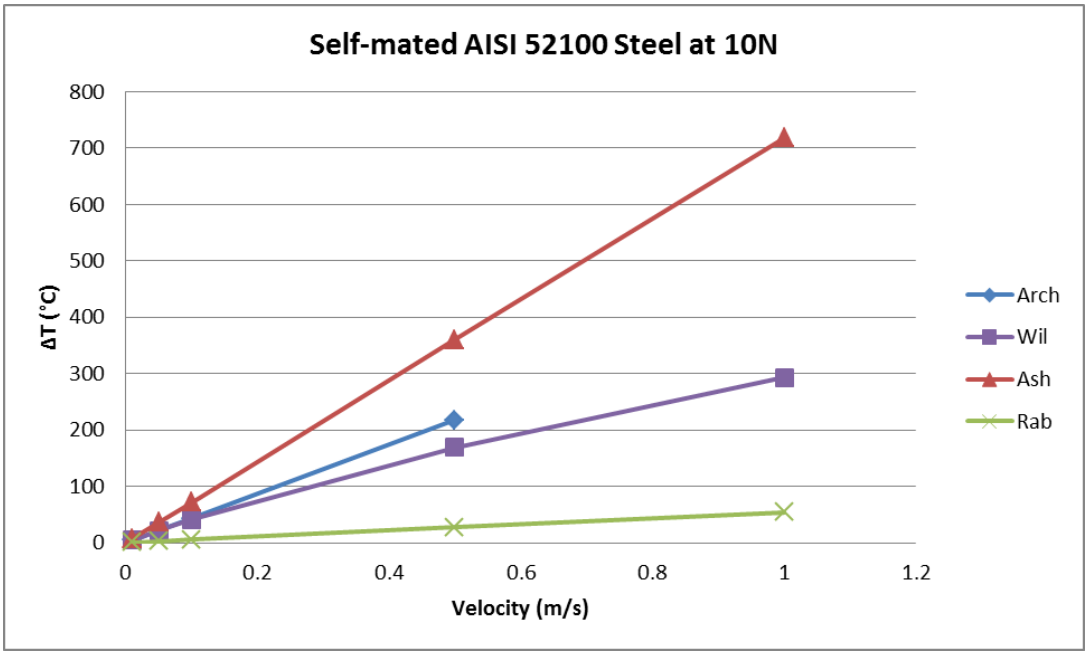

Figure 1. Friction-Induced Temperature Rise for Self-Mated AISI 52100 Steel at 10 N load.

5.9 *Graphical comparison of models for AISI 52100 Steel on Silicon Nitride Ceramic*

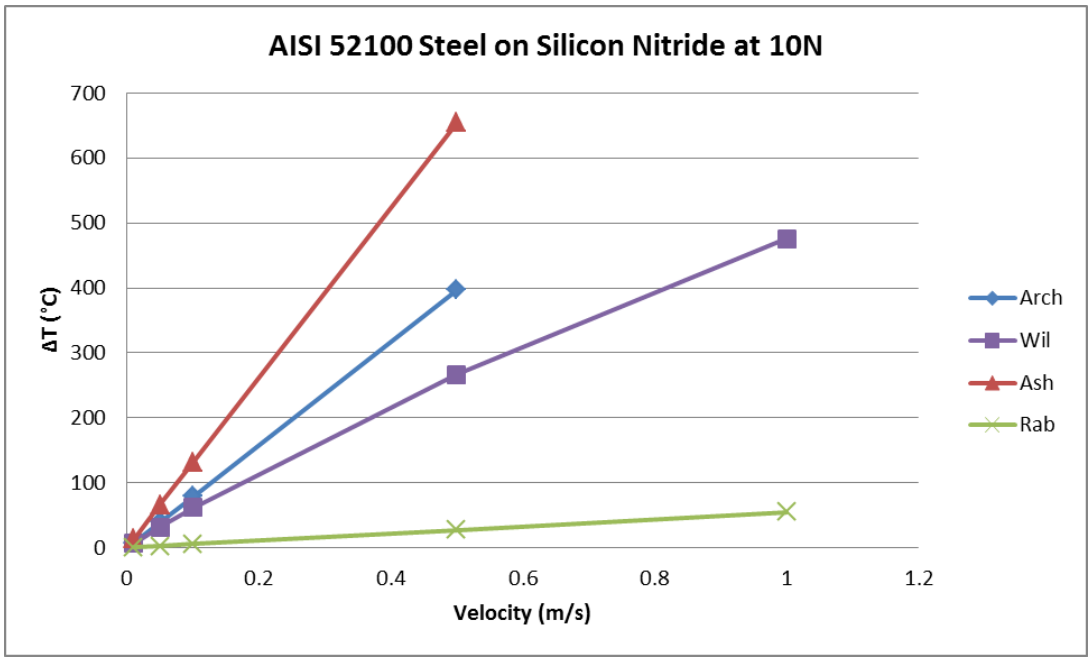

Figure 2. Friction-Induced Temperature Rise for AISI 52100 sliding on Silicon Nitride at 10 N load.

5.10 *Graphical comparison of models for AISI 52100 Steel on CDA 932 Bronze*

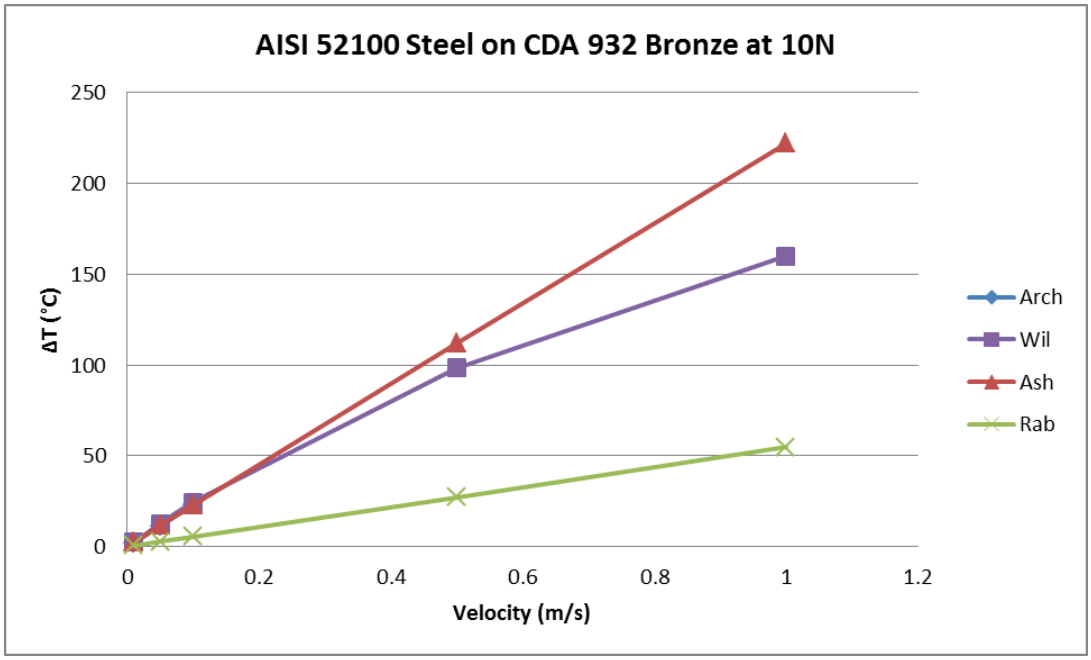

Figure 3. Friction-Induced Temperature Rise for AISI 52100 sliding on CDA 932 Bronze at 10 N load. Archard model data are superimposed on the Wil and Ash results up to 0.1 m/s, but above that speed values exceed the melting point of the bronze and are not plotted.

6.0 Summary and Conclusions

Four models to predict the temperature rise for dry, solid-on-solid frictional heating were compared. Each produced different results given similar inputs, indicating the importance of setting the proper initial conditions and assumptions. The Archard model assumes a heat flow relationship that causes a discontinuous jump in predicted frictional heating under conditions of high speed and load. The Wilsdorf model ignores this heat flow relationship, but assumes instead additional sources of heat loss as well as additional non-frictional sources of heat, causing its results to be lower than those of the Archard in the case of self-mated materials (the Archard model seems to be less accurate for dissimilar material combinations and will have more erratic results). Unlike the other models, the Lim-Ashby model places a great deal of importance upon the contact properties and is significantly affected by small differences in the presumed physical arrangement and surface topography, such as the linear diffusion distance and asperity radius. The approximation given by the Rabinowicz back-of-the envelope calculation is at best a very rough estimate.

In light of the assumptions made in the four models, some conclusions about their relationships may be drawn. Firstly, under the self-mated material combinations that the Archard model assumes, the results will always be greater than those of the Wilsdorf model, which allows more ways to dissipate the heat, but otherwise follows a nearly identical set of equations. Secondly, the Lim-Ashby model will vary

greatly based on the contact properties when compared to the other models; if a typical set of contact conditions is selected, however, the Lim-Ashby model will agree with the Archard and Wilsdorf models over a relatively large range of velocities and loads. Lastly, the Rabinowicz rough estimate is generally unreliable, especially in high load and high speed situations where it greatly underestimates the temperature rise predicted by other models.

7.0 References

1. J. F. Archard (1958/1959) "The Temperatures of Rubbing Surfaces," *Wear*, Vol 2, pp. 438-455.
2. H. Blok (1937) "Theoretical Study of Temperature Rise at Surfaces of Actual Contact under Oiliness Lubricating Conditions," *Proc. General Discussions on Lubrications and Lubricants,* Vol 2, Institute of Mechanical Engineers, London, pp. 222-235.
3. J.C. Jaeger (1942) "Moving Sources of Heat and Temperature at Sliding Contacts," *J. Proc. R. Soc. (NSW),* Vol 76, pp. 203-224.